



<http://www.diva-portal.org>

This is the published version of a paper published in *Advanced Electronic Materials*.

Citation for the original published paper (version of record):

Auroux, E., Sandström, A., Larsen, C., Zäll, E., Lundberg, P. et al. (2021)
Evidence and Effects of Ion Transfer at Active-Material/Electrode Interfaces in
Solution-Fabricated Light-Emitting Electrochemical Cells
Advanced Electronic Materials, 7(8): 2100253
<https://doi.org/10.1002/aelm.202100253>

Access to the published version may require subscription.

N.B. When citing this work, cite the original published paper.

Permanent link to this version:

<http://urn.kb.se/resolve?urn=urn:nbn:se:umu:diva-185329>

Evidence and Effects of Ion Transfer at Active-Material/Electrode Interfaces in Solution-Fabricated Light-Emitting Electrochemical Cells

Etienne Auroux, Andreas Sandström, Christian Larsen, Erik Zäll, Petter Lundberg, Thomas Wågberg, and Ludvig Edman*

The light-emitting electrochemical cell (LEC) allows for energy- and cost-efficient printing and coating fabrication of its entire device structure, including both electrodes and the single-layer active material. This attractive fabrication opportunity is enabled by the electrochemical action of mobile ions in the active material. However, a related and up to now overlooked issue is that such solution-fabricated LECs commonly comprise electrode/active-material interfaces that are open for transfer of the mobile ions, and it is herein demonstrated that a majority of the mobile anions in a common spray-coated active material can transfer into a spray-coated poly(3,4-ethylenedioxythiophene):poly(styrene-sulfonate) (PEDOT:PSS) positive electrode during LEC operation. Since it is well established that the mobile ion concentration in the active material has a profound influence on the LEC performance, this significant ion transfer is an important factor that should be considered in the design of low-cost LEC devices that deliver high performance.

diode (OLED), requires an ultraprecise multilayer structure for high-performance operation, which is difficult to realize with high-throughput coating and printing. The light-emitting electrochemical cell (LEC) is a less-investigated alternative to the OLED, which can deliver a good light-emission performance from a much simpler device architecture, in the form of a single-layer active material sandwiched between two air-stable electrodes.^[9–16]

The origin for the functionality of the simpler LEC architecture is the existence of mobile ions blended with the OSC in the active material.^[17–19] When a voltage is applied between the two electrodes during LEC operation, these mobile ions redistribute in a rather fascinating manner. First, a small number of negative anions and positive cations drift to accumulate

close to the positive anode and negative cathode, respectively, for the establishment of two efficient injection layers (so-called electric double layers). Thereafter, the remaining ions drift to electrostatically compensate the first injected holes and electrons for the formation of a p-type transport layer next to the anode and an n-type transport layer next to the cathode. Subsequently injected holes and electrons can recombine under the emission of light in the region in between the p-type and n-type regions, the so-called p-n junction. Accordingly, the initially uniform active material has, through the ion motion, transformed into a functional five-layer structure that allows for efficient injection, transport and recombination of electrons and holes.^[20]


This unique electrochemical doping operation has paved the way for the fabrication of functional LEC devices with a wide range of scalable coating and printing methods, including spray^[21,22] and slot-die^[23] coating, and inkjet^[24,25] and gravure^[26] printing. These studies have also contributed with practical guidelines as regards to the functional solution-based deposition of the LEC active material, which include the importance of a fast drying process to suppress a detrimental phase separation between the OSC and the electrolyte and the accumulation of ambient dust,^[21] as well as the appropriate tuning of the rheological properties of the active-material ink—by, e.g., polymeric weight, salt concentration, and solvent dilution—for the selected printing and coating method.^[25–27] Unfortunately, the

1. Introduction

Thin-film electroluminescent devices based on organic semiconductors (OSCs) are often praised for their potential for fabrication by energy-efficient and low-cost printing and coating,^[1–8] but currently no such all-solution-processed technology is on the market. One reason is that the current thin-film electroluminescent technology in vogue, the organic light-emitting

E. Auroux, Dr. C. Larsen, E. Zäll, Dr. P. Lundberg, Prof. T. Wågberg, Prof. L. Edman
 Department of Physics
 Umeå University
 Umeå SE-90187, Sweden
 E-mail: ludvig.edman@umu.se

Dr. A. Sandström, Dr. C. Larsen, Prof. L. Edman
 LunaLEC AB, Linnaeus väg 24
 Umeå SE-90187, Sweden

 The ORCID identification number(s) for the author(s) of this article can be found under <https://doi.org/10.1002/aelm.202100253>.

© 2021 The Authors. Advanced Electronic Materials published by Wiley-VCH GmbH. This is an open access article under the terms of the Creative Commons Attribution-NonCommercial-NoDerivs License, which permits use and distribution in any medium, provided the original work is properly cited, the use is non-commercial and no modifications or adaptations are made.

DOI: 10.1002/aelm.202100253

corresponding number of studies on the functional printing and coating deposition of the electrodes in LEC devices is markedly lower,^[23,28–32] and it is a particular concern that the knowledge on how such deposition should be designed and executed for high-performance operation is poor.

In this study we address this issue through a systematic comparison and analysis of the performance of LEC devices equipped with evaporated electrodes and solution-processed electrodes. We find that an up-to-now overlooked issue originates in that the solution-processed electrodes can form interfaces with the active material that are open to ion transfer during LEC operation. Since it is well-established that the effective mobile ion concentration in the active material strongly affects the LEC performance,^[33–38] it is clear that this “loss” of ions into the open solution-processed LEC electrodes is a significant factor that needs to be considered for the rational design of high-performance LEC devices. We specifically establish that a majority of the anions in a commonly employed active material transfers into a spray-coated poly(3,4-ethylenedioxythiophene):poly(styrene-sulfonate) (PEDOT:PSS) positive electrode, where they effectuate for additional p-type doping of PEDOT:PSS. A direct consequence of this ion transfer is that the required ion concentration for peak performance is much higher in LEC devices equipped with open solution-processed electrodes than compact evaporated electrodes, and in the herein studied devices the optimum ion concentration is found to increase by a factor of four to ten, depending on the thickness of the open electrode.

2. Results and Discussion

A principle goal of this study is to investigate whether there are fundamental differences in LEC operation when employing conventional compact evaporated electrodes in comparison to solution-processed electrodes that commonly are more open and porous. To this end, we have fabricated and characterized three different types of LEC devices that are distinguished by the top-electrode selection: i) A conventional “closed-electrode-LEC” featuring a compact Al top electrode fabricated by thermal vacuum evaporation; ii) a “thin-open-electrode-LEC” fabricated with a 350-nm-thin layer of spray-coated PEDOT:PSS as the top electrode; and iii) a “thick-open-electrode-LEC” equipped with a 1- μm -thick layer of spray-coated PEDOT:PSS as the top electrode. The selection of the word “closed” or “open” reflects the anticipated lack or availability, respectively, of free-volume voids of the size of molecular entities such as ions within the top electrode.

The bottom electrode was invariably transparent and compact indium tin oxide (ITO), and it was biased positive for the closed-electrode-LEC and negative for the open-electrode-LECs. This is because Al has been demonstrated to be electrochemically unstable at positive bias in similar LEC devices,^[39,40] whereas the originally p-type doped PEDOT:PSS can lose its required electrode conductivity by dedoping under negative bias.^[41,42] The active material comprised a blend of the fluorescent conjugated polymer Super Yellow and the electrolyte tetrahexylammonium tetrafluoroborate (THABF₄), and it was designed to be all-hydrophobic in order to remain intact during the solution-based spray-coating deposition of the hydrophilic

PEDOT:PSS ink. The Al electrode is highly reflective, with the simulated average reflectance in the visible range being 84%,^[40] whereas the PEDOT:PSS electrodes are highly transparent, with the thin and thick PEDOT:PSS electrodes featuring a transmittance at 550 nm of 89% and 72%, respectively.^[30] As the luminance was measured at the ITO side of the device, we multiplied the measured luminance by a factor of two for the open-electrode-LECs in order to compensate for that a significant fraction of the generated light is leaking out through the transparent PEDOT:PSS top electrode without being detected.

Figure 1a,b presents the temporal evolution of the voltage and the luminance, respectively, during driving by a constant current density of 100 A m⁻² for the closed-electrode-LEC (solid black circles), the thin-open-electrode-LEC (red crosses), and the thick-open-electrode-LEC (open green diamonds) with a 4 mass% ion concentration in the active material. The consistent observation for all investigated LEC devices is that the voltage decreases with time during the initial constant-current driving (see also Figure S1 in the Supporting Information). This characteristic behavior of a functional LEC is due to the ion-migration-induced formation of electric double layers (EDLs) at the two electrode interfaces, which causes improved electronic injection, and the subsequent electrochemical doping of the organic semiconductor, p-type at the positive anode and n-type at the negative cathode, which results in improved bulk electronic transport. The latter electrochemical doping process eventually results in the formation of a p-n junction doping structure in the active material. An increasing luminance during the initial operation is a further consistent observation for all devices (see Figure 1b; Figure S1, Supporting Information), which is essentially due to improved electron and hole recombination effectuated by the formation of the p-n junction doping structure in the active material.^[10,43–45] We can therefore draw the conclusion that both the closed-electrode-LEC and the two open-electrode-LECs exhibit the baseline criteria for functional LEC operation.

Figure 1c,d presents a summary of the measured minimum voltage and the peak luminance, respectively, as a function of the ion concentration. We mention that a few of the open-electrode-LEC devices with low ion concentration reached the voltage compliance of 21 V before reaching peak luminance, and that these data therefore are excluded from Figure 1d. More importantly, Figure 1c shows that all three device structures exhibit a decrease in the minimum voltage with increasing ion concentration, which is a direct manifestation of that each ion can contribute to one electrochemical doping event, and that this doping increases the effective conductance of the LEC device. Moreover, we find that the highest peak luminance of the two open-electrode-LECs is on par with that of the more conventional closed-electrode-LEC, which is evidence for that the spray-coating deposition of the top PEDOT:PSS electrode has resulted in functional devices.

Interestingly, we also observe a couple of distinct and consistent differences between the three device structures. First, the minimum voltage at a set ion concentration is consistently higher for the open-electrode-LECs than for the closed-electrode-LEC, with the highest voltage being measured for the thick-open-electrode-LEC (as indicated by the arrow in Figure 1c). The latter observation excludes the trivial explanation that a higher sheet resistance of the top electrode is the origin to the

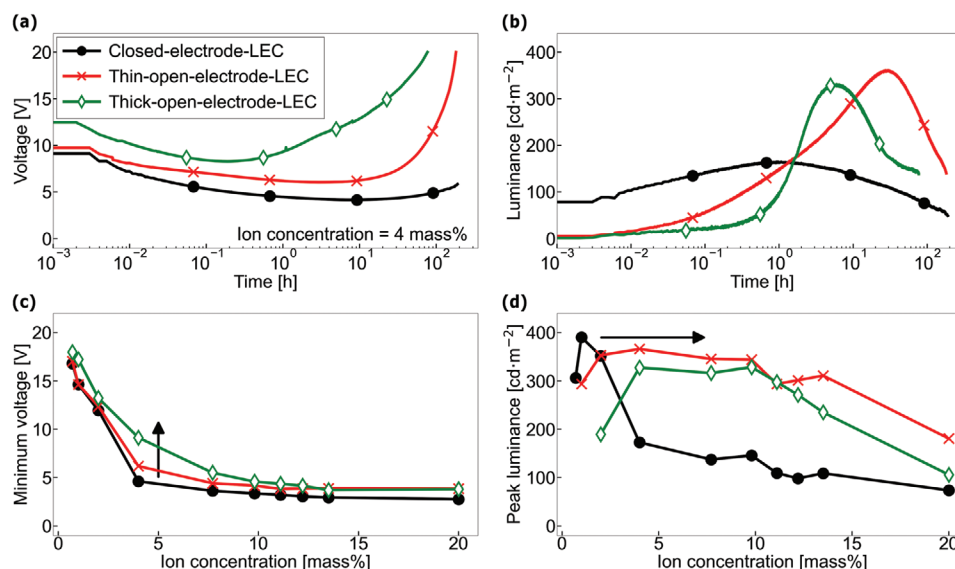


Figure 1. The temporal evolution of a) the voltage and b) the luminance during driving by a current density of 100 A m^{-2} for the three different LEC architectures identified in the inset in (a). The THABF_4 ion concentration in the active material is 4 mass%. The dependency on the ion concentration in the active material for c) the minimum voltage and d) the peak luminance for the three device architectures identified in the inset in (a). The data presented in (c,d) are the average values for ≥ 4 devices.

higher voltage, since the thicker PEDOT:PSS electrode features a lower sheet resistance than the thinner PEDOT:PSS electrode ($65 \text{ vs } 220 \Omega \text{ square}^{-1}$). Second, the ion concentration at which the highest peak luminance is measured is notably lower at 1 mass% for the closed-electrode-LEC than for the two open-electrode-LECs at 4–10 mass%, as indicated by the arrow in Figure 1d.

Our hypothesis is that these distinguishing observations can be explained by that some of the ions in the active material are migrating into the PEDOT:PSS top electrode during the operation of the open-electrode-LECs, whereas a corresponding ion transfer is effectively prohibited in the closed-electrode-LEC by the compact nature of its Al top electrode. This ion transfer will result in a decrease of the ion concentration in the active material, which in turn will lower the (average) doping concentration in the active material at steady state, i.e., at the time of the lowest voltage. A lowered doping concentration is concomitant with a lowered conductance, which will result in that the voltage required to drive a set current through the active material will increase. The fact that the minimum voltage is larger for the thick-open-electrode-LEC than for the thin-open-electrode-LEC in Figure 1c implies that the relative magnitude of this ion transfer, quite reasonably, increases with the thickness of the open electrode.

The same ion-transfer effect can also rationalize why the peak luminance is observed to shift to a higher ion concentration for the open-electrode-LECs compared to the closed-electrode-LEC (see arrow in Figure 1d). It has been firmly established that an optimum ion concentration exists for each LEC active material, at which a delicate balance between the positive and the detrimental effects of the doping is attained, as discussed in detail in, e.g., refs. [34,36,37,46]. Thus, if a significant fraction of the ions in the active material is being “lost” by the transfer into the open electrode, this optimum initial ion concentration in the active material needs to be increased in order to attain the doping-balancing criterion.

A relevant question that then follows is what is the effect for the PEDOT:PSS electrode when ions from the active material are entering into it during LEC operation? In order to answer this question, we have performed systematic and correlated electrochemical and optical experiments on spray-coated PEDOT:PSS electrodes. Figure 2a,b presents a set of linear sweep voltammetry (LSV) traces, distinguished by the different end potentials, recorded during electrochemical reduction and oxidation, respectively, of a pristine PEDOT:PSS electrode in contact with the THABF_4 electrolyte. The fact that the traces exhibit very good overlap demonstrate the good repeatability of the LSV experiment.

The semiconducting PEDOT polymer is originally p-type doped, with polymeric PSS anions serving as the electrostatically compensating negative counter-ions. The reduction of the PEDOT:PSS electrode depicted in Figure 2a is thus anticipated to correspond to “dedoping” of the p-type doped PEDOT by hole extraction, which is electrostatically compensated by injection of THA cations from the LSV electrolyte. Note that the polymeric PSS anions (and the neutral PSS based polymers) are expected to be effectively immobile within the PEDOT:PSS film because of their large size.

The total number of added or removed redox charges per PEDOT repeat unit during one such LSV scan can be estimated by integrating the LSV current (I) over time and using the following equation

$$\frac{n_{\text{redox charge}}}{n_{\text{PEDOT}}} = \frac{M_{\text{PEDOT}}}{N_A \cdot \rho \cdot A \cdot d \cdot X_{\text{PEDOT:PSS}}^{\text{PEDOT}}} \cdot \frac{1}{e} \int I dt \quad (1)$$

where M_{PEDOT} is the molecular mass of one PEDOT repeat unit ($=140 \text{ g mol}^{-1}$), N_A the Avogadro number, ρ the density of PEDOT:PSS ($\approx 1.0 \times 10^6 \text{ g m}^{-3}$),^[47,48] A the LSV-active area of the

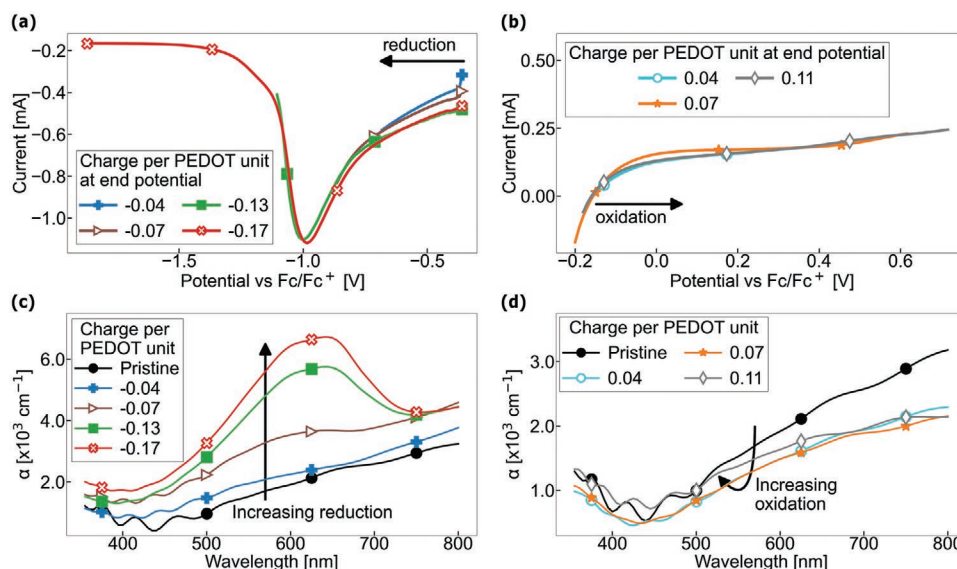


Figure 2. Linear sweep voltammograms recorded on pristine 1- μm -thick PEDOT:PSS films during a) electrochemical reduction and b) electrochemical oxidation. The traces are distinguished by the different end potentials, and the scan rate was 0.05 V s^{-1} . The corresponding absorption spectra measured after the voltammograms on c) the reduced PEDOT:PSS films and d) the oxidized PEDOT:PSS films. The inset values for the charge concentration injected into the PEDOT:PSS films were calculated by integrating the redox current in (a,b) and dividing by the PEDOT:PSS film volume.

PEDOT:PSS electrode ($=2.8 \times 10^{-4} \text{ m}^2$), d the thickness of the PEDOT:PSS electrode ($\approx 1075 \text{ nm}$), $X_{\text{PEDOT:PSS}}^{\text{PEDOT}}$ the mass fraction of PEDOT in the PEDOT:PSS electrode (≈ 0.29),^[49–51] and e the elementary charge.

The derived values for the removed redox charge per PEDOT repeat unit during the LSV reduction scans are presented in the inset of Figure 2a, and we find that the reduction scan with the highest negative end potential of -1.9 V versus the Fc/Fc⁺ reference electrode (marked by open red crosses) has resulted in the removal of 0.17 redox charges per PEDOT repeat unit. For the preservation of electroneutrality within the PEDOT:PSS films, this mandates a corresponding influx of 0.17 THA cations per PEDOT repeat unit from the LSV electrolyte.

However, the operation of the open-electrode-LECs, as depicted in Figure 1, concerns the PEDOT:PSS electrode under positive bias, which renders the LSV oxidation experiment in Figure 2b more relevant. We calculate the total injected oxidation charge during the three different LSV oxidation traces displayed in Figure 2b with the aid of Equation (1), and we find that it ranges between 0.04 and 0.11 injected redox charges per PEDOT repeat unit, as specified in the inset. This oxidation reaction must, for electroneutrality reason, be balanced by a corresponding influx of the same amount of BF₄ anions into the PEDOT:PSS from the LSV electrolyte.

Now, a critical question is whether this oxidation of the PEDOT:PSS electrode results in further p-type doping of the already p-type doped PEDOT or whether it results in non-conductivity-enhancing “over-oxidation”^[52–54] reactions (which could, e.g., result in a cleaving of the conjugated-polymer chain or the formation of a sulfoxide entity on the sulfur atom of the thiophene group).^[55] In response to this query, we measured the change in absorption of the PEDOT:PSS electrode following the electrochemical reactions, since it is

well-established that the PEDOT semiconductor decreases its absorption in the visible range markedly with increasing conductivity-enhancing p-type doping.^[41,42,56] We specifically measured the transmittance (T) of the PEDOT:PSS electrode as a function wavelength (λ) before and directly after each LSV trace; and by neglecting reflection, we can calculate the absorption coefficient (α) as a function of λ for the different PEDOT:PSS films with the aid of the Beer–Lambert law

$$\alpha(\lambda) = \frac{-\log_{10}(T(\lambda))}{d} \quad (2)$$

where d is the film thickness. Figure 2c shows that the absorption within the visible range increases monotonously with increasing reduction of the PEDOT:PSS electrode. This is in perfect agreement with that the visible absorption of PEDOT:PSS increases with decreasing p-type doping,^[41,42,56] and our results thus reveal that the originally p-type doped PEDOT can be dedoped by (at least) 0.17 positive charges per PEDOT repeat unit, and that the pristine PEDOT:PSS electrode consequently exhibits a p-type doping level of at least 0.17 dopants per PEDOT repeat unit.

Of more relevance for the operation of the open-electrode-LECs is that Figure 2d reveals that the absorption of the PEDOT:PSS electrode within the visible range is further decreased when the film is electrochemically oxidized by 0.04 charges per PEDOT repeat unit, but that this trend is halted at higher oxidation levels. The conclusion is thus that the originally p-type doped PEDOT:PSS electrode can be further electrochemically p-type doped by 0.04 holes (and 0.04 BF₄ anions) per PEDOT repeat unit, but that the injection of additional oxidation charge results in an “overoxidation” reaction. This implies that the lower limit for the p-type doping capacity of the PEDOT:PSS electrode is 0.21 dopants per PEDOT repeat unit,

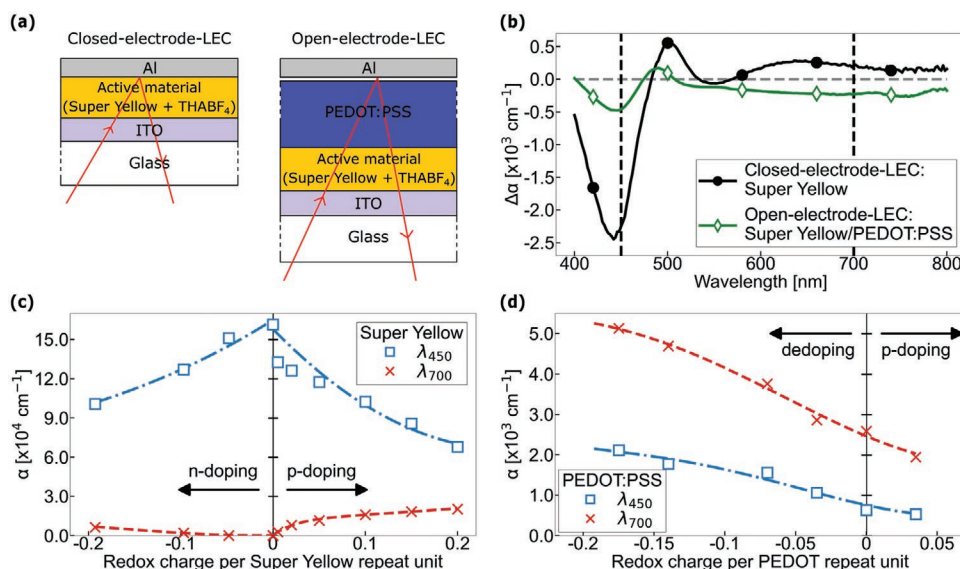


Figure 3. a) A schematic depicting the probing light beam (red line with arrow) during the measurement of the absorption coefficient for the closed-electrode-LEC (left) and the thick-open-electrode-LEC (right). b) The measured change in the absorption coefficient as a function of wavelength during LEC operation for the closed-electrode-LEC (solid black circles) and the thick-open-electrode-LEC (open green diamonds). The thickness of the active material was 200 nm, the thickness of the PEDOT:PSS electrode was 1000 nm, the THABF₄ ion concentration was 10 mass%, and the LECs were driven by a constant current density of 200 A m⁻². The absorption coefficient α for c) Super Yellow (in the active material) and d) PEDOT:PSS as a function of injected electrochemical redox charge at $\lambda = 450$ nm (open blue squares) and $\lambda = 700$ nm (red crosses). Note that pristine Super Yellow is undoped, while the PEDOT in pristine PEDOT:PSS is p-type doped. The data corresponding to overoxidation of PEDOT:PSS have been removed for clarity.

and that one in five PEDOT units then harbors a hole and a compensating anion.

A direct verification of that the solution-processed PEDOT:PSS electrode indeed can be additionally p-type doped is provided by in situ measurements of its change in absorption during device operation. Figure 3a is a schematic presentation of our employed setup, depicting the path of the probing illumination beam (red line with arrow) in the absorption experiments on the closed-electrode-LEC (left) and the open-electrode-LEC (right). The detailed measurement procedure is presented in the Supporting Information and visualized in Figure S2 in the Supporting Information.

Figure 3b presents the measured change of the absorption coefficient between the pristine state and the steady state ($\Delta\alpha$) for the closed-electrode-LEC (solid black circles) and for the thick-open-electrode-LEC (open green diamonds). The time for steady state is defined as the time of the minimum voltage, at which we estimate that all ions have participated in doping as the device conductivity is at its highest value. Since the glass substrate and the bottom ITO electrode remain invariant during these experiments, the measured change in absorption for the compact-electrode-LEC is solely due to changes in the active material, specifically to changes in the Super Yellow semiconductor, whereas the change in absorption for the open-electrode-LEC is due to the combined change in absorption of the Super Yellow in the active material and of the PEDOT semiconductor in the PEDOT:PSS top electrode.

We call attention to two specific observations in Figure 3b. i) The closed-electrode-LEC features a strong drop in absorption at 450 nm ($\Delta\alpha$ negative) during operation, which is significantly lowered for the thick-open-electrode-LEC; ii) The

closed-electrode-LEC exhibits an increase in absorption at 700 nm ($\Delta\alpha$ positive), which is shifted to a decrease for the thick-open-electrode-LEC. In order to explain these results, Figure 3c,d presents the evolution of the absorption coefficient at 450 nm (α_{450}) and 700 nm (α_{700}) with injected redox charge for Super Yellow and for PEDOT:PSS, respectively. The former data were gleaned from a publication by Lanz and coworkers,^[57] while the latter were extracted from Figure 2. We remind that the injection of negative (positive) redox charge into the pristine undoped Super Yellow results in n-type (p-type) doping, while the corresponding situation for the pristine p-type doped PEDOT:PSS is that the injection of negative (positive) redox charge results in removal (addition) of p-type doping.

With these reference data at hand, we find that the situation is as expected for the closed-electrode-LEC. More specifically, the strong negative value for $\Delta\alpha$ at 450 nm is due to the formation of p-type and n-type doping of the Super Yellow semiconductor in the active material during LEC operation, which strongly bleach the short-wavelength π - π^* transition of Super Yellow at 450 nm, whereas the positive value for $\Delta\alpha$ at 700 nm is because the same doping reactions result in the formation of broad polaron absorption bands at 700 nm.^[57,58]

The analysis of the effects following the addition of the PEDOT:PSS layer in the thick-open-electrode-LEC is interesting. At the shorter wavelength of 450 nm, the PEDOT:PSS addition results in a marked diminishing of the negative $\Delta\alpha$ change during LEC operation (compare open green diamonds with solid black circles in Figure 3b). This observation can be explained by that a significant fraction of the p-type doping of Super Yellow in the closed-electrode-LEC has transformed into additional p-type doping of PEDOT:PSS in the

open-electrode-LEC, and that p-type doping of PEDOT:PSS results in a much smaller absorption decrease at 450 nm than the p-type doping of Super Yellow that it replaced. A comparison of the absolute change of α_{450} for Super Yellow with p-type doping (Figure 3c, open blue squares) with that of PEDOT:PSS with additional p-type doping (Figure 3d, open blue squares) provides support for that this is indeed the case.

At the longer wavelength of 700 nm, $\Delta\alpha$ shifts from being positive with only Super Yellow as the absorption-active species in the closed-electrode-LEC to become negative with both Super Yellow and PEDOT:PSS in the thick-open-electrode-LEC. This observation is in qualitative agreement with that Super Yellow features an increasing absorption at 700 nm with p-type doping (Figure 3c, red crosses), while PEDOT:PSS exhibits a decreasing absorption with p-type doping at the same wavelength (Figure 3d, red crosses). Moreover, the fact that $\Delta\alpha$ at 700 nm turns negative for the thick-open-electrode-LEC implies that the decrease in absorption following the additional p-type doping of PEDOT:PSS must be larger than the increase in absorption following the doping of Super Yellow in the active material. A comparison of the absolute change of α_{700} during doping of Super Yellow with that of additional p-type doping of PEDOT:PSS implies that a majority of the p-type doping of Super Yellow in the closed-electrode-LEC must have transformed into p-type doping of PEDOT:PSS in the thick-open-electrode-LEC. An obvious consequence is that a majority of the negative BF_4 anions in the active material has transferred into the PEDOT:PSS electrode during the operation of thick-open-electrode-LEC.

In this context it is interesting to calculate the additional p-type doping level of the PEDOT:PSS electrode that would result if all anions from the active material transfers into it during LEC operation, using the below equation

$$\begin{aligned}\sigma_{\text{PEDOT}}^{\text{p-type,add}} &= \frac{n_{\text{BF}_4}}{n_{\text{PEDOT}}} = \frac{m_{\text{BF}_4}}{M_{\text{BF}_4}} \cdot \frac{M_{\text{PEDOT}}}{m_{\text{PEDOT}}} \\ &= \frac{m_{\text{BF}_4}}{m_{\text{THABF}_4}} \cdot \frac{m_{\text{THABF}_4}}{m_{\text{AM}}} \cdot \frac{m_{\text{AM}}}{X_{\text{PEDOT:PSS}}^{\text{PEDOT}} \cdot m_{\text{PEDOT:PSS}}} \cdot \frac{M_{\text{PEDOT}}}{M_{\text{BF}_4}} \quad (3) \\ &\approx \frac{m_{\text{THABF}_4}}{m_{\text{AM}}} \cdot \frac{d_{\text{AM}}}{X_{\text{PEDOT:PSS}}^{\text{PEDOT}} \cdot d_{\text{PEDOT:PSS}}} \cdot \frac{M_{\text{PEDOT}}}{M_{\text{THABF}_4}}\end{aligned}$$

where n_{BF_4} is the number of anions in the active material, n_{PEDOT} the number of PEDOT repeat units in the PEDOT:PSS electrode, m the mass, M the molecular weight, d_{AM} and $d_{\text{PEDOT:PSS}}$ the thickness of the active material and the PEDOT:PSS electrode, respectively, and the assumption is that the density of the active material is the same as that of the PEDOT:PSS electrode.

For the thick-open-electrode LEC with an ion concentration of 10 mass% investigated in Figure 3b we find that $\sigma_{\text{PEDOT}}^{\text{p-type,add}}$ is equal to 0.022 additional p-type dopants per PEDOT repeat unit, which is well below the upper limit for the maximum additional p-type doping capacity of the herein investigated PEDOT:PSS of 0.04 p-type dopants per PEDOT repeat unit (see Figure 2 and related discussion). Thus, it is in principle possible that all BF_4 anions has transferred into the thick PEDOT:PSS electrode during LEC operation, and we note that the data presented in Figure 3b implies that at least a majority of the BF_4

anions has made the transfer. For the thin-electrode-LEC at 10 mass% ion concentration, the corresponding outcome for a complete transfer of all BF_4 anions from the active material into the thinner PEDOT:PSS electrode is that $\sigma_{\text{PEDOT}}^{\text{p-type,add}}$ is equal to 0.062 additional p-type dopants per PEDOT repeat unit, which is above the threshold for additional p-type doping. This implies that only a fraction (<65%) of the BF_4 anions has made the transfer or alternatively that some overoxidation of PEDOT has taken place for the thin-electrode-LEC with 10 mass% ion concentration.

At this point we remind of the results in Figure 1d which revealed that the ion concentration for peak luminance was shifted from 1 mass% for the closed-electrode-LEC to 4 mass% for the thin-open-electrode LEC and to 10 mass% for the thick-open-electrode-LECs. This finding is in line with that a majority of the BF_4 anions indeed have made the transfer into the PEDOT:PSS electrode in the herein studied devices at steady-state operation. However, it should also be acknowledged that the ion concentration for optimum LEC operation is expected to be altered when the emission zone (i.e., the p-n junction) is shifted towards an electrode interface,^[59] since this will also alter exciton-electrode quenching, exciton-polaron quenching,^[37,46,60–62] and the influence of cavity effects.^[63–66] Nevertheless, the consistent overall picture that emerges in this study is that a majority of the anions in the active material has migrated into the relatively thick (compared to the active material) PEDOT:PSS positive anode during LEC operation, and that this transfer has a profound influence on the device operation.

In the same context, we note with interest that it is common to include a relatively thin (typically ≈ 20 – 40 nm) spin-coated layer of PEDOT:PSS in between the ITO anode and the active material in conventional closed-electrode-LECs.^[67–69] The motivation for the inclusion of this “intermediate layer” in LEC devices has, to our knowledge, not been systematically studied, but the herein presented results imply that a similar transfer of anions into the PEDOT:PSS layer could be expected, albeit at lower relative magnitude (since the PEDOT:PSS layer is thinner than the active material). This in turn suggests that the PEDOT:PSS layer becomes additionally p-type doped, and that the p-n junction as a consequence is shifted away from the reflective Al cathode towards the anode. Since it is well-established that excitons are severely quenched by a nearby metallic electrode, such as Al,^[70,71] this suggests that (at least a part of) the motivation for including a thin intermediate PEDOT:PSS layer in a closed-electrode-LEC device could be for shifting the p-n junction to a more effective location for emission.

3. Conclusion

We demonstrate that solution-fabricated LECs can feature active material/electrode interfaces that are open for ion transfer during device operation, and that a direct consequence of this ion transfer is that a significant fraction of the ions in the active material migrates into the open electrodes during the initial device operation. More specifically, we show that a vast majority of the anions in a commonly employed active material has transferred into a spray-coated PEDOT:PSS positive electrode during the initial LEC operation, and that the consequences

are that the PEDOT:PSS electrode is further p-type doped and that the initial ion concentration in the active material for peak performance increases by a factor of four to ten depending on the thickness of the PEDOT:PSS electrode. Accordingly, our study pinpoints an up-to-now overlooked issue as regards to the operation of printed and coated LEC devices, and as such provides a practical and rational guideline for how low-cost thin-film LEC devices shall be designed for high-performance operation.

4. Experimental Section

The conjugated poly(para-phenylene vinylene) co-polymer termed Super Yellow (catalogue number: PDY-132, Merck, GER) and the ionic liquid tetrahexylammonium tetrafluoroborate (THABF₄, Merck, GER) were separately dissolved in cyclohexanone in a concentration of 8 and 10 g L⁻¹, respectively, through stirring on a magnetic hotplate at 70 °C for >24 h. These master inks were blended into a blend solution with a THABF₄ ion concentration that was systematically varied between 0.7 and 20 mass%. The blend solutions were stirred for >4 h on a magnetic hotplate at 70 °C, and thereafter diluted with 450 volume% tetrahydrofuran (THF, Merck, GER) under ambient air to form the active-material inks.

Pre-patterned ITO coated glass substrates (area: 30 × 30 mm², ITO thickness = 145 nm, Thin Film Devices, US) were cleaned by sequential 10 min ultrasonic treatment in detergent (Extran MA 01, Merck, GER), distilled water, acetone (VWR, GER), and isopropanol (VWR, GER), and thereafter dried at 120 °C for ≥24 h. The active-material ink was spray-sintered on top of the ITO-coated substrates, kept at 60 °C, using a spray box (LunaLEC AB, SWE). The spray parameters were: N₂ gas pressure = 450 kPa, ink flow rate = 4 mL min⁻¹, number of sweeps = 4, spray time = 80 s. The thickness of the dry active material was 200 nm, as measured with a stylus profilometer (Dektak XT, Bruker, US).

For the “open-electrode-LECs,” two PEDOT:PSS inks were prepared by diluting a commercial PEDOT:PSS dispersion (Clevios SV3, Heraeus, GER) with either 400 or 200 volume% of methanol, followed by ≥45 min sonication in an ultrasonic bath. The PEDOT:PSS ink under study was spray-coated directly on top of the dry active material using the spray box, with the substrate maintained at 60 °C. The spray parameters were: N₂ gas pressure = 410 kPa, ink flow rate = 4 mL min⁻¹, number of sweeps = 3, spray time = 60 s. A shadow mask defined the shape of the PEDOT:PSS top electrodes during the spray coating, and the overlap of the patterned PEDOT:PSS top electrodes and the patterned ITO bottom electrodes defined four 2 × 2 mm² LEC devices on one substrate. Immediately after the spray-coating of the PEDOT:PSS electrodes, the devices were dried at 120 °C for ≥4 min on a hotplate. The dry thickness of the PEDOT:PSS electrode was either 350 or 1000 nm, as determined by the 400 or 200 volume% methanol dilution of the original PEDOT:PSS ink, and as measured with the stylus profilometer. The device featuring the 350-nm thin PEDOT:PSS top electrode is termed the “thin-open-electrode-LEC,” whereas the device equipped with the 1000-nm thick PEDOT:PSS top electrode is called the “thick-open-electrode-LEC.”

For the “closed-electrode-LEC,” a set of four Al top electrodes was deposited on top of the dry active material through a shadow mask by thermal evaporation under high vacuum (*p* = 0.3 mPa). The overlap between the patterned Al top electrodes and the patterned ITO bottom electrodes defined four 2 × 2 mm² devices on one substrate.

The LEC devices were driven and measured with a computer-controlled setup (OLED lifetime tester M6000 PMX, McScience, KOR), with the voltage compliance set to 21 V. All LEC devices were driven by a constant current density of 100 A m⁻². The device characterization of the non-encapsulated LECs was executed in a N₂-filled glovebox ([O₂] <1 ppm, [H₂O] <1 ppm), whereas their entire

fabrication was executed under ambient air, with the exceptions of the active-material ink preparation that was performed in a N₂-filled glovebox ([O₂] <1 ppm, [H₂O] <1 ppm) and the deposition of the Al top electrodes.

The electrochemical interrogation of the PEDOT:PSS electrodes was carried out with linear sweep voltammetry (LSV). The LSV setup comprised a computer-controlled potentiostat (Autolab PGSTAT302, software GPES, NLD), and the working electrode was a PEDOT:PSS film (thickness: 1000 nm; area: 14 × 20 mm²) spray-coated on top of an ITO-coated glass substrate, a Pt rod was the counter electrode, a Ag rod was the quasi-reference electrode, and 0.1 M THABF₄ in anhydrous CH₃CN was the electrolyte. The scan rate was 0.05 V s⁻¹.

Immediately after the electrochemical interrogation, the PEDOT:PSS electrode was transferred to a spectrophotometer (Lambda 1050, PerkinElmer, USA) for a transmittance measurement. The transmittance of the large-area LEC devices (emission area: 30 × 30 mm², glass substrate area: 50 × 50 mm²) before and after LEC operation was measured in a spectrophotometer equipped with a 150 mm integrating sphere (Lambda 1050, PerkinElmer, USA). The absorption coefficient of the PEDOT:PSS electrodes and the large-area LEC devices was calculated from the measured transmittance and the film thickness, and neglecting the effects of reflectance, using the Beer–Lambert law, as specified in Equation (2).

Supporting Information

Supporting Information is available from the Wiley Online Library or from the author.

Acknowledgements

The authors acknowledge financial support from the Swedish Research Council, the Swedish Energy Agency, Carl Tryggers stiftelse, Kempestiftelserna, Stiftelsen Olle Engkvist Byggmästare, Interreg Nord, Region Västerbotten, and Bertil & Britt Svenssons stiftelse för belysningsteknik.

Conflict of Interest

The authors declare no conflict of interest.

Data Availability Statement

The data that support the findings of this study are available from the corresponding author upon reasonable request.

Keywords

active-material design, electrode electrochemistry, ion transfer, light-emitting electrochemical cell, PEDOT:PSS, solution fabrication

Received: March 12, 2021

Revised: May 18, 2021

Published online: June 16, 2021

- [1] F. Z. Wang, J. F. Fan, X. N. Dang, X. Fan, P. Wang, X. H. Wan, D. C. Zou, S. H. Kim, D. N. Lee, B. H. Kim, *J. Appl. Phys.* **2008**, 103,104509.

- [2] J. Bharathan, Y. Yang, *Appl. Phys. Lett.* **1998**, 72, 2660.
- [3] S. C. Chang, J. Liu, J. Bharathan, Y. Yang, J. Onohara, J. Kido, *Adv. Mater.* **1999**, 11, 734.
- [4] B. Park, O. E. Kwon, S. H. Yun, H. G. Jeon, Y. H. Huh, *J. Mater. Chem. C* **2014**, 2, 8614.
- [5] R. R. Sondergaard, M. Hosel, F. C. Krebs, *J. Polym. Sci., Part B: Polym. Phys.* **2013**, 51, 16.
- [6] K. Hong, Y. K. Kwon, J. Ryu, J. Y. Lee, S. H. Kim, K. H. Lee, *Sci. Rep.* **2016**, 6, 29805.
- [7] A. C. Arias, J. D. MacKenzie, I. McCulloch, J. Rivnay, A. Salleo, *Chem. Rev.* **2010**, 110, 3.
- [8] G. Hernandez-Sosa, N. Bornemann, I. Ringle, M. Agari, E. Dorsam, N. Mechau, U. Lemmer, *Adv. Funct. Mater.* **2013**, 23, 3164.
- [9] Y.-X. Liu, R.-H. Yi, C.-H. Lin, Z.-P. Yang, C.-W. Lu, H.-C. Su, *J. Mater. Chem. C* **2020**, 8, 14378.
- [10] Q. B. Pei, G. Yu, C. Zhang, Y. Yang, A. J. Heeger, *Science* **1995**, 269, 1086.
- [11] X. W. Meng, M. Z. Chen, R. B. Bai, L. He, *Inorg. Chem.* **2020**, 59, 9605.
- [12] D. Gets, M. Alahbakhshi, A. Mishra, R. Haroldson, A. Papadimitratos, A. Ishteev, D. Saranin, S. Anoshkin, A. Pushkarev, E. Danilovskiy, S. Makarov, J. D. Slinker, A. A. Zakhidov, *Adv. Opt. Mater.* **2021**, 9, 2001715.
- [13] R. Bai, X. Meng, X. Wang, L. He, *Adv. Funct. Mater.* **2021**, 31, 2007167.
- [14] G. X. Yu, C. H. Lin, Y. X. Liu, R. H. Yi, G. Y. Chen, C. W. Lu, H. C. Su, *Chem.-Eur. J.* **2019**, 25, 13748.
- [15] E. Fresta, J. M. Carbonell-Vilar, J. Y. Yu, D. Armentano, J. Cano, M. Viciano-Chumillas, R. D. Costa, *Adv. Funct. Mater.* **2019**, 29, 1901797.
- [16] J. E. Namanga, N. Gerlitzki, A.-V. Mudring, *Adv. Funct. Mater.* **2017**, 27, 1605588.
- [17] Q. B. Pei, Y. Yang, G. Yu, C. Zhang, A. J. Heeger, *J. Am. Chem. Soc.* **1996**, 118, 3922.
- [18] J. M. Leger, *Adv. Mater.* **2008**, 20, 837.
- [19] E. Fresta, M. A. Monclus, M. Bertz, C. Ezquerro, J. M. Molina-Aldareguia, J. R. Berenguer, M. Kunimoto, T. Homma, R. D. Costa, *Adv. Opt. Mater.* **2020**, 8, 2000295.
- [20] S. Tang, L. Edman, *Top. Curr. Chem.* **2016**, 374, 40.
- [21] A. Sandström, A. Asadpoordarvish, J. Enevold, L. Edman, *Adv. Mater.* **2014**, 26, 4975.
- [22] A. Asadpoordarvish, A. Sandström, C. Larsen, R. Bollström, M. Toivakka, R. Österbacka, L. Edman, *Adv. Funct. Mater.* **2015**, 25, 3238.
- [23] A. Sandström, H. F. Dam, F. C. Krebs, L. Edman, *Nat. Commun.* **2012**, 3, 1002.
- [24] E. M. Lindh, A. Sandström, L. Edman, *Small* **2014**, 10, 4148.
- [25] G. Mauthner, K. Landfester, A. Kock, H. Bruckl, M. Kast, C. Stepper, E. J. W. List, *Org. Electron.* **2008**, 9, 164.
- [26] G. Hernandez-Sosa, S. Tekoglu, S. Stolz, R. Eckstein, C. Teusch, J. Trapp, U. Lemmer, M. Hamburger, N. Mechau, *Adv. Mater.* **2014**, 26, 3235.
- [27] G. Hernandez-Sosa, R. Eckstein, S. Tekoglu, T. Becker, F. Mathies, U. Lemmer, N. Mechau, *Org. Electron.* **2013**, 14, 2223.
- [28] P. Matyba, H. Yamaguchi, M. Chhowalla, N. D. Robinson, L. Edman, *ACS Nano* **2011**, 5, 574.
- [29] J. Zimmermann, S. Schliske, M. Held, J.-N. Tisserant, L. Porcarelli, A. Sanchez-Sanchez, D. Mecerreyes, G. Hernandez-Sosa, *Adv. Mater. Technol.* **2019**, 4, 1800641.
- [30] E. Auroux, A. Sandström, C. Larsen, P. Lundberg, T. Wågberg, L. Edman, *Org. Electron.* **2020**, 84, 105812.
- [31] P. Matyba, H. Yamaguchi, G. Eda, M. Chhowalla, L. Edman, N. D. Robinson, *ACS Nano* **2010**, 4, 637.
- [32] Z. Shu, F. Kemper, E. Beckert, R. Eberhardt, A. Tünnemann, *Mater. Today: Proc.* **2017**, 4, 5039.
- [33] S. van Reenen, P. Matyba, A. Dzwilewski, R. A. J. Janssen, L. Edman, M. Kemerink, *Adv. Funct. Mater.* **2011**, 21, 1795.
- [34] M. Diethelm, Q. Grossmann, A. Schiller, E. KCapp, S. Jenatsch, M. Kawecki, F. Nüesch, R. Hany, *Adv. Opt. Mater.* **2019**, 7, 1801278.
- [35] J. F. Fang, Y. L. Yang, L. Edman, *Appl. Phys. Lett.* **2008**, 93, 063503.
- [36] J. Fang, P. Matyba, L. Edman, *Adv. Funct. Mater.* **2009**, 19, 2671.
- [37] S. Tang, A. Sandström, P. Lundberg, T. Lanz, C. Larsen, S. van Reenen, M. Kemerink, L. Edman, *Nat. Commun.* **2017**, 8, 1190.
- [38] J. Gao, *ChemPlusChem* **2018**, 83, 183.
- [39] J. H. Shin, P. Matyba, N. D. Robinson, L. Edman, *Electrochim. Acta* **2007**, 52, 6456.
- [40] J. Xu, A. Sandström, E. M. Lindh, W. Yang, S. Tang, L. Edman, *ACS Appl. Mater. Interfaces* **2018**, 10, 33380.
- [41] S. Sakamoto, M. Okumura, Z. Zhao, Y. Furukawa, *Chem. Phys. Lett.* **2005**, 412, 395.
- [42] Q. Wei, M. Mukaida, Y. Naitoh, T. Ishida, *Adv. Mater.* **2013**, 25, 2831.
- [43] D. J. Dick, A. J. Heeger, Y. Yang, Q. B. Pei, *Adv. Mater.* **1996**, 8, 985.
- [44] S. B. Meier, S. van Reenen, B. Lefevre, D. Hartmann, H. J. Bolink, A. Winnacker, W. Sarfert, M. Kemerink, *Adv. Funct. Mater.* **2013**, 23, 3531.
- [45] D. B. Rodovsky, O. G. Reid, L. S. C. Pingree, D. S. Ginger, *ACS Nano* **2010**, 4, 2673.
- [46] S. van Reenen, R. A. J. Janssen, M. Kemerink, *Adv. Funct. Mater.* **2015**, 25, 3066.
- [47] A. Lenz, H. Kariis, A. Pohl, P. Persson, L. Ojamäe, *Chem. Phys.* **2011**, 384, 44.
- [48] A. Elschner, S. Kirchmeyer, W. Lovenich, U. Merker, K. Reuter, *PEDOT: Principles and Applications of an Intrinsically Conductive Polymer*, CRC Press, Boca Raton **2010**.
- [49] S. He, M. Mukaida, K. Kirihaara, L. Lyu, Q. Wei, *Polymers* **2018**, 10, 1065.
- [50] S. Zhang, P. Kumar, A. S. Nouas, L. Fontaine, H. Tang, F. Cicoira, *APL Mater.* **2015**, 3, 014911.
- [51] W. Cai, T. Österberg, M. J. Jafari, C. Musumeci, C. Wang, G. Zuo, X. Yin, X. Luo, J. Johansson, M. Kemerink, *J. Mater. Chem. C* **2020**, 8, 328.
- [52] A. Zykwiniska, W. Domagala, B. Pilawa, M. Lapkowski, *Electrochim. Acta* **2005**, 50, 1625.
- [53] X. Du, Z. Wang, *Electrochim. Acta* **2003**, 48, 1713.
- [54] J. Fan, S. S. Rezaie, M. Facchini-Rakovich, D. Gudi, C. Montemagno, M. Gupta, *Org. Electron.* **2019**, 66, 148.
- [55] M. A. Kamensky, S. N. Eliseeva, G. Láng, M. Ujvári, V. V. Kondratiev, *Russ. J. Electrochem.* **2018**, 54, 893.
- [56] S. Garreau, G. Louarn, J. P. Buisson, G. Froyer, S. Lefrant, *Macromolecules* **1999**, 32, 6807.
- [57] T. Lanz, E. M. Lindh, L. Edman, *J. Mater. Chem. C* **2017**, 5, 4706.
- [58] N. Kaihovirta, A. Asadpoordarvish, A. Sandström, L. Edman, *ACS Photonics* **2014**, 1, 182.
- [59] M. Diethelm, A. Schiller, M. Kawecki, A. Devižis, B. Blülle, S. Jenatsch, E. Knapp, Q. Grossmann, B. Ruhstaller, F. Nüesch, R. Hany, *Adv. Funct. Mater.* **2020**, 30, 1906803.
- [60] P. Lundberg, Y. Tsuchiya, E. M. Lindh, S. Tang, C. Adachi, L. Edman, *Nat. Commun.* **2019**, 10, 5307.
- [61] F. AlTal, J. Gao, *Org. Electron.* **2015**, 18, 1.
- [62] S. Jenatsch, M. Regnat, R. Hany, M. Diethelm, F. Nüesch, B. Ruhstaller, *ACS Photonics* **2018**, 5, 1591.
- [63] E. M. Lindh, P. Lundberg, T. Lanz, L. Edman, *Sci. Rep.* **2019**, 9, 10433.
- [64] E. M. Lindh, P. Lundberg, T. Lanz, J. Mindemark, L. Edman, *Sci. Rep.* **2018**, 8, 6970.
- [65] T. W. Wang, H. C. Su, *Org. Electron.* **2013**, 14, 2269.

- [66] C.-Y. Cheng, C.-W. Wang, J.-R. Cheng, H.-F. Chen, Y.-S. Yeh, H.-C. Su, C.-H. Chang, K.-T. Wong, *J. Mater. Chem. C* **2015**, 3, 5665.
- [67] A. Mishra, S. DiLuzio, M. Alahbakhshi, A. C. Adams, M. H. Bowler, J. Moon, Q. Gu, A. A. Zakhidov, S. Bernhard, J. D. Slinker, *Chem. Mater.* **2021**, 33, 1201.
- [68] Y. X. Liu, R. H. Yi, C. H. Lin, Z. P. Yang, C. W. Lu, H. C. Su, *J. Mater. Chem. C* **2020**, 8, 14378.
- [69] S. Tang, P. Murto, X. Xu, C. Larsen, E. Wang, L. Edman, *Chem. Mater.* **2017**, 29, 7750.
- [70] J. Rafols-Ribe, E. Gracia-Espino, S. Jenatsch, P. Lundberg, A. Sandstrom, S. Tang, C. Larsen, L. Edman, *Adv. Opt. Mater.* **2021**, 9, 2001405.
- [71] A. L. Burin, M. A. Ratner, *J. Phys. Chem. A* **2000**, 104, 4704.